

LETTERS

White organic light-emitting diodes with fluorescent tube efficiency

Sebastian Reineke¹, Frank Lindner¹, Gregor Schwartz¹, Nico Seidler¹, Karsten Walzer¹, Björn Lüssem¹ & Karl Leo¹

The development of white organic light-emitting diodes¹ (OLEDs) holds great promise for the production of highly efficient large-area light sources. High internal quantum efficiencies for the conversion of electrical energy to light have been realized^{2–4}. Nevertheless, the overall device power efficiencies are still considerably below the 60–70 lumens per watt of fluorescent tubes, which is the current benchmark for novel light sources. Although some reports about highly power-efficient white OLEDs exist^{5,6}, details about structure and the measurement conditions of these structures have not been fully disclosed: the highest power efficiency reported in the scientific literature is 44 lm W⁻¹ (ref. 7). Here we report an improved OLED structure which reaches fluorescent tube efficiency. By combining a carefully chosen emitter layer with high-refractive-index substrates^{8,9}, and using a periodic outcoupling structure, we achieve a device power efficiency of 90 lm W⁻¹ at 1,000 candelas per square metre. This efficiency has the potential to be raised to 124 lm W⁻¹ if the light outcoupling can be further improved. Besides approaching internal quantum efficiency values of one, we have also focused on reducing energetic and ohmic losses that occur during electron–photon conversion. We anticipate that our results will be a starting point for further research, leading to white OLEDs having efficiencies beyond 100 lm W⁻¹. This could make white-light OLEDs, with their soft area light and high colour-rendering qualities, the light sources of choice for the future.

To turn a white OLED into a power-efficient light source, three key parameters must be addressed: the internal electroluminescence quantum efficiency must be close to one (high internal quantum efficiency), a high fraction of the internally created photons must escape to the forward hemisphere (high outcoupling efficiency) and the energy loss during electron–photon conversion should be small (low operating voltage). The internal quantum efficiency and the outcoupling efficiency are combined in the external quantum efficiency (EQE).

The use of phosphors allows 100% internal quantum efficiency, because both the singlet and triplet states (generated at a ratio of 1:3 owing to their multiplicity) are directed to the emitting triplet state¹⁰. For power-efficient white OLEDs, an additional challenge is that high-energy phosphors demand host materials with even higher triplet energies to confine the excitation to the emitter¹¹. Taking exciton binding energy and singlet–triplet splitting into account, the use of such host materials considerably increases the transport gap and therefore the operating voltage. For these reasons, blue fluorescent emitters are widely used to complete the residual phosphor-based emission spectrum^{2,12,13}; this, however, either reduces the internal quantum efficiency or requires blue emitters with special properties¹⁴. Whenever OLEDs are built in a standard substrate emitting architecture, the outcoupling efficiency is approximately 20%. The remaining 80% of the photons are trapped in organic and substrate modes in equal

amounts¹⁵. Hence, the greatest potential for a substantial increase in EQE and power efficiency is to enhance the light outcoupling.

Here we present an OLED structure that combines a novel concept for energy-efficient photon generation with improved outcoupling. The key feature of the OLED layer structure is the positioning of the blue phosphor within the emission layer and its combination with a carefully chosen host material: energetically, the triplet energy of the blue emitter material is in resonance with its host so that the blue phosphorescence is not accompanied by internal triplet energy relaxation before emission. The exciton formation region is at the interface of a double-emission-layer structure¹⁶. The blue host–guest system is surrounded by red and green sublayers of the emission layer to harvest unused excitons. For holes and electrons, the emission layer is nearly barrier-free until they reach the region of exciton formation, which keeps the operating voltage low. The outermost layers in contact with the electrodes are chemically p- and n-doped, which reduces ohmic losses to a negligible level¹⁶.

A close-up of the emission layer (Fig. 1a) shows the highest occupied molecular orbital (HOMO) and lowest unoccupied molecular orbital (LUMO)—the energy levels at which charge transport occurs—and the triplet energies of all materials. The latter essentially define the exciton distribution within the multilayer emission layer and, consequently, the emission spectrum and device efficiency. Holes and electrons are injected without facing any energy barrier into the emission layer from NPB to TCTA:Ir(MDQ)₂(acac) and from TPBi to TPBi:Ir(ppy)₃, respectively. (See Methods Summary for materials composition.) Here, holes are transported directly within the HOMO level of the emitter owing to its high concentration (10 wt%). Both carriers will accumulate at the double-emission-layer interface, forming excitons nearby. The different sublayers are separated by thin intrinsic interlayers of the corresponding host material to decouple the sublayers from unwanted energy transfer. Here, 2 nm is sufficient to suppress Förster-type transfer because the typical Förster radii for Ir complexes¹⁷ are less than 2 nm. Excitons created in the blue region on host or dopant have various decay channels.

The transfer rate k_{b-r} to the red emitter is strongly reduced with the introduction of the high-triplet-energy TCTA interlayer, restricting diffusive exciton migration¹⁸. Owing to their resonant triplet energies of 2.6 eV (see Fig. 2a), triplet excitons are free to move within the TPBi:Ir(ppy)₃ layer, resulting in a back-energy transfer rate k_{BT} accompanied by a delayed component in the decay of the emitting species¹⁹. This system cannot maintain the intrinsically high quantum yield of Ir(ppy)₃, so the blue region is followed by an Ir(ppy)₃-doped region, retaining high efficiency by diffusively harvesting host excitons, represented by a rate of transfer from blue to green of k_{b-g} . The interlayer between blue and green ensures that solely diffusive energy exchange contributes to k_{b-g} , as Förster-type transfers are suppressed¹⁷.

We now discuss the exciton dynamics in this emission layer. First, we present direct proof of the back-energy transfer k_{BT} in a complete

¹Institut für Angewandte Photophysik, George-Bähr-Strasse 1, D-01062 Dresden, Germany.

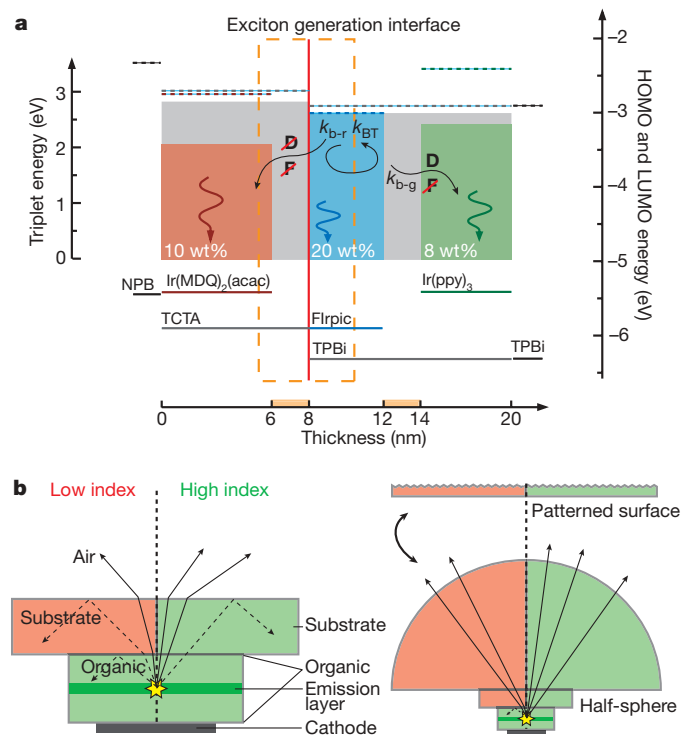


Figure 1 | Energy level diagram and light modes in an OLED. **a**, Lines correspond to HOMO (solid) and LUMO (dashed) energies; filled boxes refer to the triplet energies. The orange colour marks intrinsic regions of the emission layer. F and D represent Förster- and Dexter-type energy exchange channels, respectively. The orange dashed box depicts the main region of exciton generation. **b**, The left panel shows a cross-section of an OLED to illustrate the light propagation. Solid lines indicate modes escaping the device to the forward hemisphere; dashed lines represent trapped modes. The right panel shows how a large half-sphere and a patterned surface can be applied to increase light-outcoupling.

device. This is followed by photoluminescence quantum yield measurements to confirm that excitons that cannot relax on FIrpic are captured diffusively by the green phosphor Ir(ppy)₃. Because k_{BT} is detected as a slow-relaxation component of the FIrpic emission, itself being one of several decay channels within the present white device structure (see Fig. 1a), we prepared an additional device B to increase the FIrpic emission, and hence k_{BT} , in the multicolour electroluminescence spectrum.

Figure 2 plots its spectrum- and time-resolved emission. In Fig. 2a, the emission is filtered using appropriate colour filters, starting with solely red emission (1) and subsequently increasing the transmission in the visible spectrum to the complete electroluminescence spectrum (5). The corresponding electroluminescence transients can be seen in Fig. 2b. First, a monoexponential decay with a time constant of 1.4 μ s is observed for the red part of the spectrum (1). With increasing transmission, a second, slower component can be observed in the electroluminescence transient with a time constant of 3.0 μ s. The spectral dependence, being directly linked to the FIrpic emission, indicates that this slow component can be exclusively attributed to k_{BT} from TPBi to FIrpic. The slow component is not seen for the blue reference device in Fig. 2b, because it comprises a TCTA:FIrpic emission layer, where excitons are confined to FIrpic¹⁹.

The photoluminescence quantum yield η_{PL} is a very reliable measure of the suitability of emitter materials because it determines the ratio between the radiative decay channel (k_r) and the sum of radiative and non-radiative (k_{nr}) relaxation. In the present system, the rate of excitons relaxing without photon emission on host sites, k_H , needs to be included, making $\eta_{PL} = k_r / (k_r + k_{nr} + k_H)$. It is known that η_{PL} decreases for a phosphor-doped host-guest system whenever the excitation is not efficiently confined to the emitting species, and in

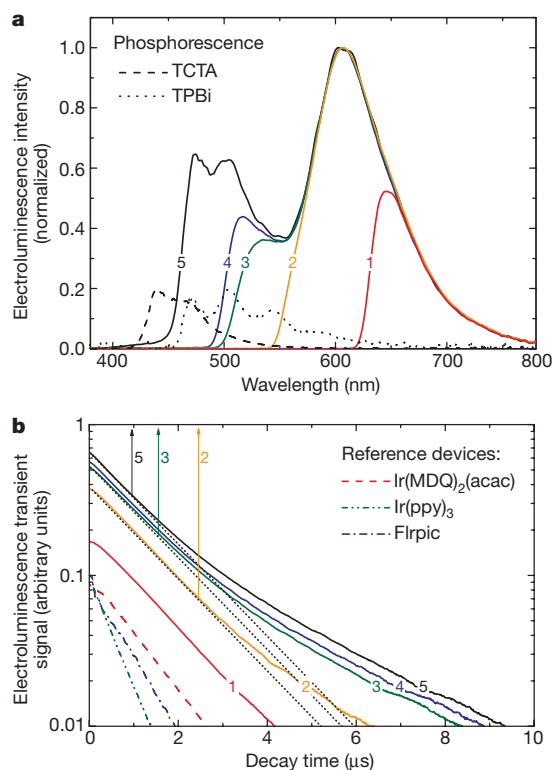


Figure 2 | Spectrum- and time-resolved electroluminescence transients. **a**, Electroluminescence spectra of device B obtained through colour filters. The spectra are numbered from solely red emission (1) to the complete emission (5). The phosphorescence spectra (at 77 K) of TCTA and TPBi are plotted. **b**, Electroluminescence decay curves of device B according to the spectrum in **a**. Arrows indicate the time at which a slower component sets in. From 1 to 5, this onset shifts to shorter times, nicely agreeing with a higher contribution of FIrpic emission. Additionally plotted are decays for blue, green and red reference devices.

most cases, this is accompanied by a back-energy transfer^{11,19}. Measurements of η_{PL} are carried out to investigate the blue to green transfer²⁰ k_{b-g} .

FIrpic is doped at 1.7 wt% either into TCTA ($T_1 = 2.8$ eV, see Fig. 2a) or TPBi, yielding very different values for η_{PL} of 81% for TCTA and 14% for TPBi, indicating that TPBi:FIrpic alone cannot be used for an efficient OLED. TCTA, with a triplet energy about 0.2 eV higher, can efficiently confine excitons to FIrpic, resulting in a very high η_{PL} (here, $k_H = 0$). By knowing the triplet decay time, $\tau = 1 / (k_r + k_{nr}) = 1.35$ μ s, for the TCTA system²¹, we can further deduce from the TPBi:FIrpic data that $k_H = 3.5 \times 10^6$ s⁻¹. The latter is roughly six times larger than the radiative rate, $k_r = 6.0 \times 10^5$ s⁻¹. It is the essence of this emission-layer design that these excitons are captured efficiently for green emission, that is, k_H feeds k_{b-g} because the Ir(ppy)₃-doped region is within the triplet diffusion length of TPBi. The photoluminescence efficiency of TPBi:FIrpic increases to 32% when the FIrpic concentration is increased to 10 wt%. This indicates that the low η_{PL} of TPBi:FIrpic is not intrinsic, but instead depends on the probability of an exciton finding a dopant site for relaxation.

The use of high-refractive-index glass substrates can substantially increase the amount of light coupled from the organic layers into the glass substrate (up to 80%)^{8,9}. In Fig. 1b, an OLED cross-section is shown to illustrate the light propagation originating in the emission layer. If we use a low-refractive-index substrate, light will face two interfaces with a step in the refractive index n . First, light will partly be reflected because of total internal reflection at the organic ($n_{org} = 1.7-1.9$)/glass substrate ($n_{low} = 1.51$) interface, forming organic modes. Second, the light entering the glass substrate is facing the glass

substrate/air ($n_{\text{air}} = 1$) interface, where total internal reflection traps it to glass modes. Although organic modes remain inside the structure and therefore cannot contribute to the total light output of the device, glass modes can be coupled out by a modification of the substrate shape (see Fig. 1b). Increasing the refractive index of the glass substrate from $n_{\text{low}} = 1.51$ to $n_{\text{high}} = 1.78$ causes the index mismatch between organic materials and substrate to vanish, enhancing light coupling into the high-refractive-index glass, so that all photons guided to organic modes by total internal reflection at the organic/glass interface in the low-refractive-index case are entering the glass substrate.

Current density and luminance are plotted versus operating voltage for all devices in Fig. 3a, with the corresponding electroluminescence spectra displayed in Fig. 3b. For both substrate types, the OLEDs achieve a brightness of $1,000 \text{ cd m}^{-2}$ slightly above 3 V; $10,000 \text{ cd m}^{-2}$ are reached below 4 V. Devices LI and HI-1 exhibit an excellent colour-rendering index of 80, similar to the best values reported for white OLEDs^{2,4,12,14}. The Commission Internationale d'Éclairage (CIE) coordinates of these devices are (0.44, 0.46) and (0.45, 0.47) for devices LI and HI-1, respectively. Because charges reach the emission layer almost without energetic barriers, the electroluminescence spectra of these devices do not depend on the brightness between 100 and $5,000 \text{ cd m}^{-2}$, which is a great improvement on many values from the literature (Supplementary Information)^{2,14,22}. Figure 4 shows the power efficiencies of devices LI and HI-1, which differ only in the use of the substrate. Unless otherwise specified, all efficiency data throughout the text refer to a luminance in forward direction of $1,000 \text{ cd m}^{-2}$.

We obtained comparable power efficiencies of 30 and 33 lm W^{-1} without outcoupling enhancement, respectively, which corresponds to 13.1% EQE for device LI and 14.4% EQE for device HI-1. With the

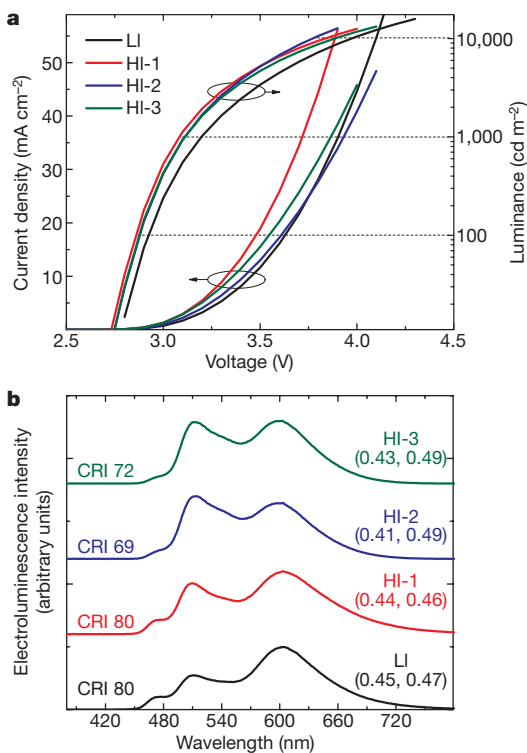


Figure 3 | Current density and luminance as a function of driving voltage and electroluminescence spectra of all devices. **a**, The data are obtained in the forward direction without outcoupling enhancement. Dashed lines indicate the brightness for 100, 1,000 and $10,000 \text{ cd m}^{-2}$. **b**, All data are obtained at $1,000 \text{ cd m}^{-2}$. Electroluminescence spectra, as displayed, are measured in direction normal to the glass substrate. In addition to the colour-rendering indices (CRI), the CIE coordinates are given. Both sets of data represent integrated values from the emission to the forward hemisphere.

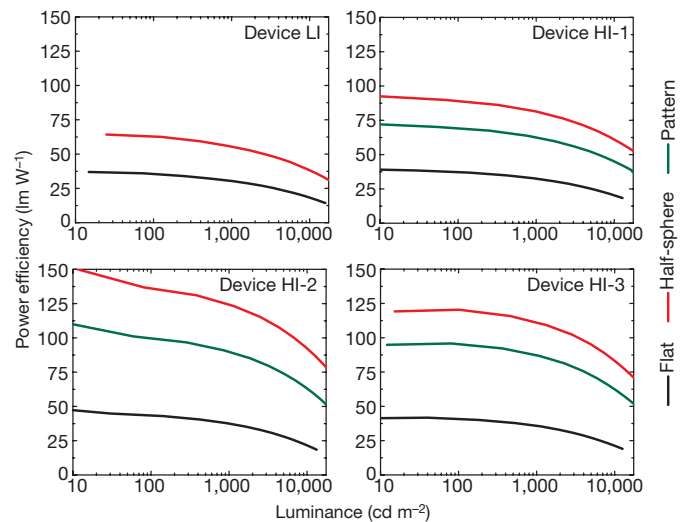


Figure 4 | Power efficiency of the white OLEDs. The power efficiencies of all devices are shown as a function of forward luminance. Black lines correspond to measurements of the planar structure (flat). The red lines are values obtained with additional index-matched half-spheres on top of the device, which indicate the maximum power efficiency because all light entering the glass substrate is coupled out to air. The green lines represent the measurements using a large-area light-outcoupling structure, that is, a periodically patterned index-matched substrate (made of Schott glass: N-LAF 21). For comparison, a typical fluorescent tube in a fixture reaches $60\text{--}70 \text{ lm W}^{-1}$.

application of an index-matched glass half-sphere, device LI reaches 55 lm W^{-1} (24% EQE), which corresponds to an increase in EQE of a factor of 1.8. This relationship drastically changes for device HI-1. Here the EQE is increased by a factor of 2.4 to 34% EQE, corresponding to 81 lm W^{-1} . One promising approach to enhance light outcoupling even for large-area devices is the use of shaped substrates, which enables the coupling of light under high angles of incidence (to the substrate surface normal). We prepared a pattern of pyramids⁹ (with period 0.5 mm) by cutting 90° grooves into a high index glass (Supplementary Information), similar to microlens arrays^{23,24}, to couple out more light. With the application of this patterned surface, device HI-1 achieves 26% EQE and 63 lm W^{-1} , already exceeding the values of device LI (with half-sphere). This result illustrates the great potential of high-refractive-index substrates.

The efficiency of organic LEDs can be increased further by placing the emission layer further away from the reflective cathode to avoid plasmonic losses to the metal^{9,25}. Plasmonic losses, where the emitting dipoles couple to surface plasmons of the reflective metal, are the dominating loss channel when the emission takes place in the proximity of the metal. Their impact steadily decreases with greater distances between the emission layer and the cathode, and drops to a negligible level for distances greater than 200 nm (ref. 25). The light extraction to air is strongly influenced by the micro-cavity formed between glass and cathode, so we observe a periodical dependence of the emitted light as a function of distance between the emission layer and the cathode with maxima at distances corresponding to constructive interference of the emission wavelength. Additionally, if the emission layer is placed in the second antinode of the reflective metal cathode, OLEDs exhibit a more direct emission, which makes the light outcoupling of substrate modes easier (Supplementary Information)²⁵.

We prepared devices HI-2 and HI-3 with 205-nm-thick and 210-nm-thick electron transport layers, respectively, to best-fit the second outcoupling maximum. Their electroluminescence spectra are shown in Fig. 3b. Unlike devices LI and HI-1, we observed strong spectral changes. Here, emission from both the blue (FIRpic) and red ($\text{Ir}(\text{MDQ})_2(\text{acac})$) regions of the emitted spectrum was decreased,

negatively affecting both the colour rendering index (which decreases to ~ 70) and CIE coordinates (which shift into the yellow region (0.41–0.43, 0.49)). These changes can clearly be attributed to the different position of the second emission maximum for all three basic emitters, with a difference of roughly 60 nm for Flrpic and Ir(MDQ)₂(acac) (Supplementary Information). This displacement from the Planck curve towards the yellow spectral range is not a large problem, and can be solved by using a deep blue phosphorescent emitter, which was not yet available to us.

The power efficiency of devices HI-2 and HI-3 can be seen in Fig. 4. Taking all substrate modes into account, these devices yield striking values of 124 and 111 lm W⁻¹, respectively. This corresponds to EQE values of 46% (HI-2) and 44% (HI-3), approaching efficiencies at which every second photon created is coupled into the forward hemisphere. Applying the pyramidal area structure to these devices, we obtain 90 lm W⁻¹ (34% EQE) and 87 lm W⁻¹ (34% EQE) for HI-2 and HI-3, respectively. These values are higher than the average power efficiency of fluorescent tubes in a fixture (60–70 lm W⁻¹). Furthermore, the novel emitter design is also characterized by an extremely small roll-off at high brightness (Supplementary Information): although it is common to state white OLED efficiency at 1,000 cd m⁻², higher brightness (2,000–5,000 cd m⁻²) could significantly reduce the size and cost of OLED lighting. Such high brightness is usually challenging owing to the pronounced roll-off in efficiency, in particular for phosphorescent emitters²⁶, but at 5,000 cd m⁻², we obtain still very high power efficiencies of 74 lm W⁻¹ (HI-2) and 73 lm W⁻¹ (HI-3).

Our results show that white OLEDs with efficiencies approaching 100 lm W⁻¹ even at high brightness are possible. For a broad application in general lighting, the lifetime issue of the blue emitters (Supplementary Information) has to be solved and the cost has to be significantly reduced, using low-cost electrode materials, thin-film encapsulation, roll-to-roll manufacturing and so on. With its potential to outperform fluorescent tubes, we think the future of white organic LEDs will be bright, not only because of their high illumination quality but also because their outstanding efficiencies will help to reduce our carbon footprint.

METHODS SUMMARY

All glass substrates were coated and structured with indium tin oxide (sheet resistance 25 Ω per square), and cleaned in an ultrasonic bath with acetone, ethanol and *iso*-propanol. All devices were fabricated by thermal evaporation in a single-chamber tool under high-vacuum conditions (base pressure $\sim 10^{-8}$ mbar). Silver top contacts were thermally evaporated without breaking the vacuum. The devices were encapsulated with an additional glass and epoxy resin in a nitrogen atmosphere before evaluation. The device area is 6.7 mm².

The main materials used have acronyms as follows. MeO-TPD: *N,N,N',N'*-tetrakis(4-methoxyphenyl)-benzidine. NPB: *N,N'*-di(naphthalen-1-yl)-*N,N'*-diphenyl-benzidine. TPBi: 2,2',2''(1,3,5-benzenetriyl) tris-(1-phenyl-1H-benzimidazole). TCTA: 4,4',4''-tris(*N*-carbazolyl)-triphenylamine. Bphen: 4,7-diphenyl-1,10-phenanthroline. Flrpic: iridium-bis-(4,6-difluorophenyl-pyridinato-*N,C2*)-picolinate. [Ir(ppy)₃]: *fac*-tris(2-phenylpyridine) iridium. Ir(MDQ)₂(acac): iridium(III)bis(2-methyl-dibenzo[f,h]quinoxaline) (acetylacetonate).

The layer sequence for the white OLED on top of a low-index substrate (device LI) is as follows: 60 nm MeO-TPD doped with 4 mol.% NDP-2 as a hole-transport layer/10 nm NPB as the electron-blocker layer/emission layer/10 nm TPBi as a hole-blocking layer/40 nm Cs-doped Bphen as an electron-transport layer/100 nm Ag cathode. Alternatively, 2,3,5,6-tetrafluoro-7,7,8,8-tetracyanoquinodimethane can be used as freely available p-dopant (Supplementary Information). The emission layer (detailed composition is shown in Fig. 1) consists of a hole-transporting layer (TCTA) and an electron-transporting host material (TPBi) partially doped with the following phosphorescent emitters: Flrpic for blue, [Ir(ppy)₃] for green and Ir(MDQ)₂(acac) for orange.

Using a high-index glass substrate (devices HI-1, HI-2 and HI-3), the transport layers are adjusted to a hole-transport layer of 45 nm to optimize the light outcoupling. The thicknesses for the electron-transport layers are 40 nm (HI-1), 205 nm (HI-2) and 210 nm (HI-3), respectively. Unlike the standard emission layer, the thickness of the TPBi:Flrpic sublayer is increased from 4 to 8 nm in device B to enhance the Flrpic emission. Device efficiencies were measured in a calibrated integrating sphere. HOMO values are obtained from ultraviolet

photoelectron spectroscopy; LUMO values are estimated from the optical gap of the material^{16,27,28}.

Full Methods and any associated references are available in the online version of the paper at www.nature.com/nature.

Received 6 December 2008; accepted 20 March 2009.

- Kido, J., Kimura, M. & Nagai, K. Multilayer white light-emitting organic electroluminescent device. *Science* **267**, 1332–1334 (1995).
- Sun, Y. *et al.* Management of singlet and triplet excitons for efficient white organic light-emitting devices. *Nature* **440**, 908–912 (2006).
- Williams, E. L., Haavisto, K., Li, J. & Jabbar, G. E. Excimer-based white phosphorescent organic light emitting diodes with nearly 100% internal quantum efficiency. *Adv. Mater.* **19**, 197–202 (2007).
- Sun, Y. & Forrest, S. R. High-efficiency white organic light emitting devices with three separate phosphorescent emission layers. *Appl. Phys. Lett.* **91**, 263503 (2007).
- Nakayama, T., Hiyama, K., Furukawa, K. & Ohtani, H. Development of phosphorescent white OLED with extremely high power efficiency and long lifetime. *SID07 Dig.* 1018–1021 (2006).
- D'Andrade, B. W. *et al.* Realizing white phosphorescent 100 lm/W OLED efficacy. *Proc. SPIE* **7051**, 70510Q (2008).
- Su, S.-J., Gonmori, E., Sasabe, H. & Kido, J. Highly efficient organic blue-and white-light-emitting devices having a carrier- and exciton-confining structure for reduced efficiency roll-off. *Adv. Mater.* **20**, 4189–4195 (2008).
- Nakamura, T., Tsutsumi, N., Juni, N. & Fujii, H. Thin-film waveguiding mode light extraction in organic electroluminescent device using high refractive index substrate. *Appl. Phys. Lett.* **97**, 054505 (2005).
- Gärtner, G. & Greiner, H. Light extraction from OLEDs with (high) index matched glass substrates. *Proc. SPIE* **6999**, 69992T (2008).
- Baldo, M. A. *et al.* Highly efficient phosphorescent emission from organic electroluminescent devices. *Nature* **395**, 151–154 (1998).
- Goushi, K., Kwong, R., Brown, J. J., Sasabe, H. & Adachi, C. Triplet exciton confinement and unconfined by adjacent hole-transport layers. *J. Appl. Phys.* **95**, 7798–7802 (2004).
- Schwartz, G., Fehse, K., Pfeiffer, M., Walzer, K. & Leo, K. Highly efficient white organic light emitting diodes comprising an interlayer to separate fluorescent and phosphorescent regions. *Appl. Phys. Lett.* **89**, 083509 (2006).
- Qin, D. & Tao, Y. White organic light-emitting diode comprising of blue fluorescence and red phosphorescence. *Appl. Phys. Lett.* **86**, 113507 (2005).
- Schwartz, G., Pfeiffer, M., Reineke, S., Walzer, K. & Leo, K. Harvesting triplet excitons from fluorescent blue emitters in white organic light-emitting diodes. *Adv. Mater.* **19**, 3672–3676 (2007).
- Greenham, N. C., Friend, R. H. & Bradley, D. D. C. Angular-dependence of the emission from a conjugated polymer light-emitting diode - implications for efficiency calculations. *Adv. Mater.* **6**, 491–494 (1994).
- He, G. *et al.* High-efficiency and low-voltage p-i-n electrophosphorescent organic light-emitting diodes with double-emission layers. *Appl. Phys. Lett.* **85**, 3911–3913 (2004).
- Kawamura, Y., Brooks, J., Brown, J. J., Sasabe, H. & Adachi, C. Intermolecular interaction and a concentration-quenching mechanism of phosphorescent Ir(III) complexes in a solid film. *Phys. Rev. Lett.* **96**, 017404 (2006).
- Reineke, S., Schwartz, G., Walzer, K. & Leo, K. Reduced efficiency roll-off in phosphorescent organic light emitting diodes by suppression of triplet-triplet annihilation. *Appl. Phys. Lett.* **91**, 123508 (2007).
- Kawamura, Y. *et al.* 100% phosphorescence quantum efficiency of Ir(III) complexes in organic semiconductor films. *Appl. Phys. Lett.* **86**, 071104 (2005).
- Greenham, N. C. *et al.* Measurement of absolute photoluminescence quantum efficiencies in conjugated polymers. *Chem. Phys. Lett.* **241**, 89–96 (1995).
- Huang, Q., Reineke, S., Walzer, K., Pfeiffer, M. & Leo, K. Quantum efficiency enhancement in top-emitting organic light-emitting diodes as a result of enhanced intrinsic quantum yield. *Appl. Phys. Lett.* **89**, 263512 (2006).
- D'Andrade, B. W., Holmes, R.-J. & Forrest, S. R. Efficient organic electrophosphorescent white-light-emitting device with a triple doped emissive layer. *Adv. Mater.* **16**, 624–628 (2004).
- Madigan, C. F., Lu, M.-H. & Sturm, J. C. Improvement of output coupling efficiency of organic light-emitting diodes by backside substrate modification. *Appl. Phys. Lett.* **76**, 081114 (2006).
- Möller, S. & Forrest, S. R. Improved light out-coupling in organic light emitting diodes employing ordered microlens arrays. *J. Appl. Phys.* **91**, 3324–3327 (2002).
- Lin, C.-H., Cho, T.-Y., Chang, C.-H. & Wu, C.-C. Enhancing light outcoupling of organic light-emitting devices by locating emitters around the second antinode of the reflective metal electrode. *Appl. Phys. Lett.* **88**, 081114 (2006).
- Baldo, M. A., Adachi, C. & Forrest, S. R. Transient analysis of organic electrophosphorescence: II. Transient analysis of triplet-triplet annihilation. *Phys. Rev. B* **62**, 10967 (2000).
- Meerheim, R. *et al.* Influence of charge balance and exciton distribution on efficiency and lifetime of phosphorescent organic light-emitting devices. *Appl. Phys. Lett.* **104**, 014510 (2008).

28. Adamovich, V. *et al.* New charge-carrier blocking materials for high efficiency OLEDs. *Org. Electron.* **4**, 77–87 (2003).

Supplementary Information is linked to the online version of the paper at www.nature.com/nature.

Acknowledgements We thank the European Commission within the sixth framework IST programme under contract IST-2002-004607 (project OLLA), for funding. We received further support via the Leibniz Prize of the Deutsche Forschungsgemeinschaft. We also thank Novaled AG, Dresden, for providing the hole-transport layer dopant NDP-2 as well as J. Förster and T. Günther for technical assistance throughout sample preparation.

Author Contributions S.R. designed the emission concept, performed the transient electroluminescence measurements, wrote the manuscript, analysed most of the data and, together with F.L., optimized and characterized the devices and designed the outcoupling structure. G.S. was involved in the development of the second maximum devices. N.S. performed the photoluminescence quantum yield measurements. K.W. and B.L. coordinated the high efficiency white OLED project. K.L. motivated this work and co-wrote the manuscript.

Author Information Reprints and permissions information is available at www.nature.com/reprints. Correspondence and requests for materials should be addressed to K.L. (leo@iapp.de).

METHODS

Reference devices. The electroluminescent decay curves of Fig. 2b correspond to the following reference samples prepared on top of standard glass coated with indium tin oxide. FIrpic consists of: 60 nm MeO-TPD:NDP-2/10 nm NPB/20 nm TCTA:FIrpic 20 wt% (ref. 21)/10 nm TPBi/50 nm Bphen:Cs/100 nm Al. Ir(ppy)₃ consists of: 60 nm MeO-TPD:NDP-2/10 nm NPB/20 nm TCTA:Ir(ppy)₃ 8 wt% (ref. 18)/10 nm TPBi/50 nm Bphen:Cs/100 nm Al. Ir(MDQ)₂(acac) consists of: 60 nm MeO-TPD:NDP-2/10 nm NPB/20 nm NPB:Ir(MDQ)₂(acac) 10 wt% (ref. 27)/10 nm TPBi/50 nm Bphen:Cs/100 nm Al.

Device evaluation. Electroluminescence spectra were recorded with a calibrated spectrometer CAS 140 CT (Instrument Systems Optische Messtechnik). Only the electroluminescence spectra as shown in Fig. 2 were recorded with a USB2000 minispectrometer (OceanOptics). All efficiency measurements were carried out in an integrating sphere (Instrument Systems Optische Messtechnik) attached to the calibrated spectrometer CAS 140 CT and a source-measure unit 2400 (Keithley Instruments). The relative efficiencies as a function of luminance were measured with a fast, calibrated photodetector in the forward direction, which were then rescaled to the values obtained with the integrating sphere. This is valid because the electroluminescence spectra do not change significantly in the displayed range of brightness. All efficiencies are given, if not stated otherwise, at a luminance of 1,000 cd m⁻² and measured in the forward direction, that is, at a normal angle of incidence for the complete device configuration, eventually

including outcoupling structures. The glass half-spheres have diameters of 18 and 15 mm for low and high refractive index, respectively. Index-matching oils of $n = 1.5$ and $n = 1.78$ were obtained from Olympus Corporation and Cargille Laboratories, respectively. Substrate edges were covered to exclude edge emission contributing to the measurement. Photoluminescence quantum yield measurements were carried out in an integrating sphere (Labsphere) using a 325 nm HeCd laser (Kimmon Electric Company) as excitation source and the USB2000 minispectrometer as detector. The set-up was calibrated using a ultraviolet/visible light source, itself calibrated with the CAS 140 CT spectrometer.

Spectroscopy. The phosphorescence spectra of TCTA and TPBi in Fig. 2a were measured at 77 K using a gated phosphorescence set-up with a 337 nm pulsed laser (MSG-SD from Lasertechnik Berlin) as excitation source. Here, the delay generator (DG 535, Stanford Research Systems), triggered with the laser pulse, gave the delay for the detection (LS 50 B spectrometer, Perkin Elmer), to separate fast and slow phosphorescence. The time and spectrally resolved measurements were carried out under electroluminescence operation. The general set-up is realized as shown previously²⁹. Using different colour filters, the transmission of the white OLED spectrum was changed. The transmitted intensity was then linked to the fast photodiode with a glass fibre to detect the time decay.

29. Reineke, S. *et al.* Measuring carrier mobility in conventional multilayer organic light emitting devices by delayed exciton generation. *Phys. Status Solidi B* **245**, 804–809 (2008).